

Magnetic-Oriented Nickel Particles and Nickel-Coated Carbon Nanotubes: An Efficient Tool for Enhancing Thermal Conductivity of PDMS Composites

*Original*

Magnetic-Oriented Nickel Particles and Nickel-Coated Carbon Nanotubes: An Efficient Tool for Enhancing Thermal Conductivity of PDMS Composites / Riccucci, G.; Romano, A.; Pezzana, L.; Tori, A.; Spriano, S.; Sangermano, M.. - In: MACROMOLECULAR CHEMISTRY AND PHYSICS. - ISSN 1022-1352. - ELETTRONICO. - (2022), p. 2200199. [10.1002/macp.202200199]

*Availability:*

This version is available at: 11583/2972925 since: 2022-11-09T10:01:21Z

*Publisher:*

WILEY-VCH VERLAG GMBH

*Published*

DOI:10.1002/macp.202200199

*Terms of use:*

This article is made available under terms and conditions as specified in the corresponding bibliographic description in the repository

*Publisher copyright*

(Article begins on next page)

# Magnetic-Oriented Nickel Particles and Nickel-Coated Carbon Nanotubes: An Efficient Tool for Enhancing Thermal Conductivity of PDMS Composites

Riccucci Giacomo, Romano Angelo, Pezzana Lorenzo, Tori Alice, Spriano Silvia, and Sangermano Marco\*

In this study, PDMS composites are thermally cured with nickel particles and nickel-coated carbon nanotubes as fillers. Both fillers are oriented with the aim to increase the thermal conductivity of the silicone polymer network, due to the formation of a continuous thermal path. Scanning electron microscopy (SEM) gives a picture of the polymer network's morphology, proving the effective alignment of the nickel particles. Rheology and attenuated total reflectance Fourier transform infrared spectroscopy (ATR-FTIR) studies confirm the full curing of the silicon network and no influence in the curing kinetics of the type and content of fillers and their orientation. Dynamic mechanical thermal analysis (DMTA) and tensile analysis show instead different thermo-mechanical behavior of the polymer network due to the presence of different fillers, different fillers percentage, and orientation. Finally, the thermal transmittance coefficient ( $k$ ) is studied by means of hot disk analysis, revealing the increment of almost 200% due to magnetic filler orientation.

## 1. Introduction

Polymeric functional materials find applications such as packaging, batteries, automotive electronic-unit controls, and 3D chips.<sup>[1,2]</sup> The excellent properties of polymer matrices such as good flexibility, low density, high impact strength, and good optical transparency made them good candidates for the next generation of high-performance electronic devices.<sup>[3]</sup> Since technology

development is leading to a high request of computational power with reduced size of the electronic devices, thermal management became crucial to support the increased demands of higher thermal performance, therefore, satisfying the high heat generation for small surfaces areas.<sup>[1,3]</sup>

In this regard, polymeric-based thermal interface materials (TIMs) are widely used to meet the challenge to dissipate and transfer the heat generated by electronic devices, guaranteeing at the same time specific optical and mechanical properties.<sup>[4]</sup> Among all, polydimethylsiloxane (PDMS) and epoxy matrices are the most used due to their distinctive characteristics, such as high flexibility and thermal stability.<sup>[5–7]</sup>

Since polymer matrices are characterized by poor thermally conductive properties, a common strategy to ensure high heat dissipation consists in the synthesis of


TIMs composites which are usually constituted by a polymer matrix and thermally conductive fillers, such as metal particles or carbon nanotubes.<sup>[8,9]</sup> It is well documented in the literature that the addition of conductive fillers in the polymer matrix is an optimal and simple approach to improve thermal conductivity.<sup>[8,10,11]</sup> Owing good thermic conductive properties, metal particles, carbon nanotubes, and fibers were widely employed for this purpose as shown in several studies.<sup>[2,12]</sup>

The main idea is to reduce the typical thermal resistance of the polymer network by alternating it with thermally conductive fillers. The final value of  $k$  (thermal conductivity coefficient) depends on the filler loading, distribution, shape, and size, as well as on the matrix-filler interface, composition, and nature of the components.<sup>[8,13]</sup>

The specific features of nanofiller such as the high surface/volume ratio, lead to a reduction of the percolation threshold achieving high thermal conductivity at low conductive filler content. For instance, carbon nanotubes (CNTs) have an extremely high  $k$  coefficient ( $6600 \text{ W mK}^{-1}$ ) and they were employed in several studies for the synthesis of high-performance thermal conductive composites.<sup>[14,15]</sup> Liu et al.<sup>[16]</sup> studied the effect of the CNTs as a filler into a silicone matrix achieving an increase of thermal conductivity of about 65% with only 3.8 w/w% of CNT. Beircuk et al.<sup>[17]</sup> studied the effect of CNT with an epoxy matrix, measuring an enhancement of thermal conductivity of 125%

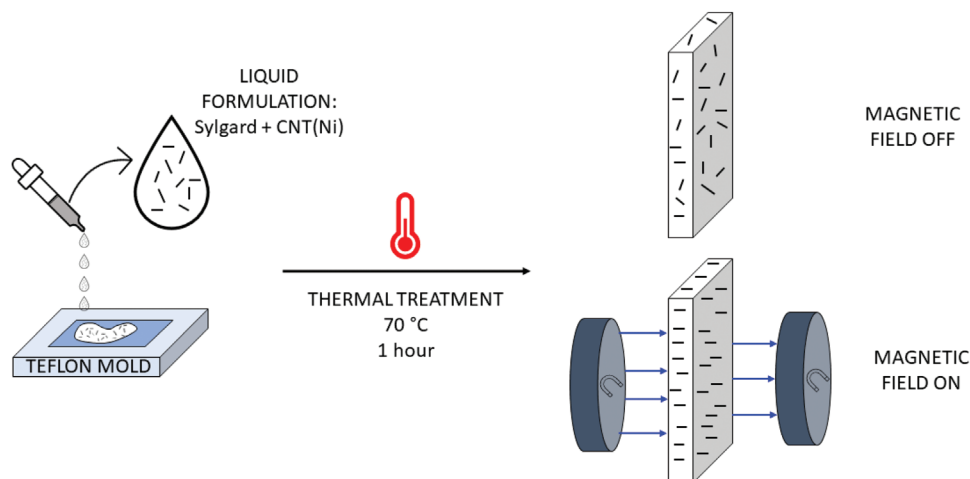
R. Giacomo, R. Angelo, P. Lorenzo, S. Silvia, S. Marco  
Department of Applied Science and Technology  
Politecnico di Torino  
Corso Duca degli Abruzzi 24, Torino 10129, Italy  
E-mail: marco.sangermano@polito.it

T. Alice  
OSAI AS S.p.A.  
Via della Cartiera 4, Parella, Torino 10010, Italy

 The ORCID identification number(s) for the author(s) of this article can be found under <https://doi.org/10.1002/macp.202200199>

© 2022 The Authors. Macromolecular Chemistry and Physics published by Wiley-VCH GmbH. This is an open access article under the terms of the Creative Commons Attribution-NonCommercial-NoDerivs License, which permits use and distribution in any medium, provided the original work is properly cited, the use is non-commercial and no modifications or adaptations are made.

DOI: 10.1002/macp.202200199



**Scheme 1.** Steps for the preparation of the different composites according to the two tested configurations.

with only 1 w/w% of added filler. The increase of the filler content results in an increase of the overall  $k$  coefficient, until a point at which the thermal conductivity of the composites becomes comparable to the one owned by thermal conductive materials. However, a limiting factor is given by the fillers' dispersion and their discontinuity inside the polymer network. Moreover, increasing the fillers' content in the aim to minimize the thermal resistance could also result in a drastic change of the mechanical properties of the polymer network.

An original strategy to limit fillers' addition and maximize their effect, lies in the formation of a continuous thermal path inside the polymer matrix. In this regard, the adoption of ferromagnetic fillers and the application of a magnetic field during the curing of the composite is an effective route for aligning the fillers and thus creating a continuous path through the composite.<sup>[18,19]</sup> Thus, an anisotropy preferential direction of the heat dissipation is established due to the continuous fillers disposition.<sup>[20,21]</sup>

Baudenne et al.<sup>[21]</sup> showed that the controlled spatial distribution of nickel particles plays a role in the thermal conductivity of the polymer composite giving an increment of  $k$  coefficient of 100% with respect to the not oriented configuration. Su et al.<sup>[22]</sup> magnetically aligned nickel particles showing that the limiting factor (also at high contents percentage) was the imperfect contact among the particles. However, they obtained a notable increase of thermal conductivity due to the alignment of the conductive particles. Kim et al.<sup>[23]</sup> designed magnetic-responsive hybrid particles depositing iron oxide nanoparticles onto a boron nitride particles surface. The fillers were then aligned and vertically disposed into an epoxy matrix creating a preferential heat-transfer direction inside the composite. The effect of orienting the particles was an increase of 100% of the  $k$  coefficient compared to a not oriented configuration. Inspired by a similar approach, Chung et al.<sup>[24]</sup> employed  $\text{Al}_2\text{O}_3\text{-Fe}_3\text{O}_4$  hybrid particles with a thermally conductive and ferromagnetic core, that were aligned through the application of a magnetic field. They reached an increment of  $k$  coefficient of 240% compared to the not oriented dispersion of the synthesized hybrid particles. CNTs were oriented employing different magnetic sensitive particles such as

Ni particles<sup>[25]</sup> or iron oxide<sup>[26]</sup> achieving good result in terms of increment of thermal conductivity.

In previous studies, we achieved an enhancement of the thermal conductivity of PDMS matrix by dispersing metal particles (copper and nickel), carbon-based materials (carbon nanotubes and carbon black), and ceramic nanoparticles (boron nitride) as thermally-conductive fillers. The influence of the filler volume, dimension, morphology, and chemical nature was studied. The results demonstrate a remarkable dependence of the final thermal properties of the composite materials from the type, size, and shape of the filler.<sup>[10]</sup>

By pursuing the research line, in this study we investigated the effect of oriented conductive fillers inside a PDMS network on thermal conductivity properties. The focus of the work is related to the possibility to achieve better thermal properties exploiting the intrinsic features of the metal particles limiting the volume addition of the filler to maintain the advantages of having a polymer matrix. Nickel metal particles and nickel coated carbon nanotubes were dispersed in the PDMS polymer matrix and composites were prepared either with an oriented and not oriented configuration of the inorganic fillers. The thermal conductivity of the composites is compared, showing a significant enhancement of the thermal conductivity by orienting the fillers inside the polymeric matrix.

## 2. Results and Discussion

The aim of this study is the enhancement of the thermal conductivity of PDMS composites by inducing an orientation of the thermal-conductive filler inside the polymeric matrix. For this reason, nickel particles and nickel coated carbon nanotubes were dispersed into a PDMS matrix, and composites were crosslinked either with not orientation of the fillers or with an oriented configuration (see **Scheme 1**). The mixed formulations were cast in a Teflon mold and then a thermal treatment was performed to achieve a crosslinked PDMS matrix. Two different filler configurations were tested: oriented and not oriented, obtained respectively with and without the application of an external magnetic field.

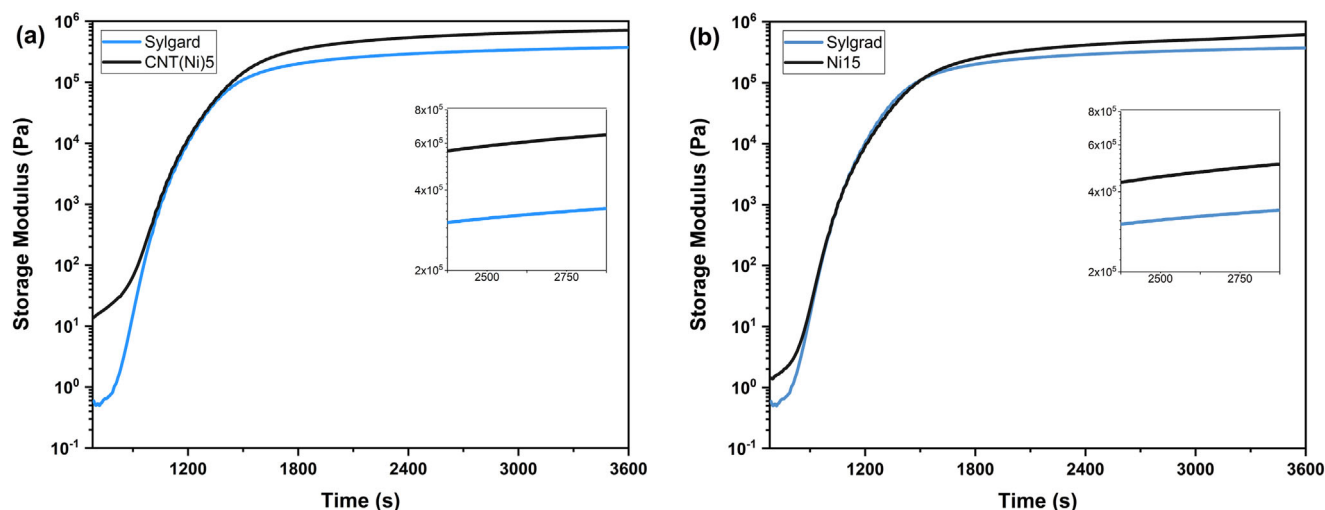


**Figure 1.** Rheology curves for the curing process (70 °C, 1 h). a) Storage modulus (Pa)/time (s) of the pristine Sylgard and the composite with 5 vol% of CNT(Ni); b) Storage modulus (Pa)/time (s) for the pristine Sylgard and composite with 15 vol% of Ni particles.

The magnetic field was kept for all the curing time to ensure an effective alignment of the filler. The composites were thermally cured for 1 h in the oven at 70 °C.

## 2.1. Thermal Curing

The curing process was followed by a rheology test with the aim to investigate the possible influence of the fillers and configuration. **Figure 1** shows the results obtained for the pristine Sylgard and for the composites with the highest amount of fillers, respectively: 15% of nickel particles (Figure 1a) and 5% of Ni-CNTs (Figure 1b). Although the measured formulations showed a similar trend of the storage modulus versus time (Figure 1), the formulation containing 5% of nickel-coated CNTs clearly shows a higher initial modulus compared to the pure Sylgard formulation and the one containing 15% of nickel particles. This is a consequence of the higher viscosity of the PDMS precursor containing Ni-CNTs fillers, and it also gives a clear indication of the formulation workability. Although the different initial modulus, no time delay was detected at the start curing point, and the reaction proceeded with a similar trend for all the formulations. A plateau is eventually reached upon 1500 s at 70 °C, which corresponds to the storage modulus of the cured samples. A higher storage modulus in the plateau region was reached for the samples containing 15% of nickel and 5% of CNTs compared to the pristine Sylgard, due to the higher mechanical rigidity of the polymer matrix containing the fillers.

In order to prove the complete curing of the polymer matrix upon the curing process (70 °C, 1 h), an ATR measurement was carried out for the pure Sylgard formulation and for the formulation containing the highest amount of fillers (15% of nickel particles) in both configurations (oriented and not oriented). **Figure 2** reports the collected ATR spectra for the formulations before and after the thermal treatment (70 °C, 1 h). As it can be noticed, the Si–H vibration peak at 2160 cm<sup>−1</sup>, disappeared completely after 1 h at 70 °C. This clearly means that the amount of fillers and their orientation did not influence the curing efficiency of PDMS.

## 2.2. Morphology Characterization

The morphologic analysis of the crosslinked composites was carried out to investigate the effective orientation of the particles within the polymeric matrix produced by the application of the external magnetic field. In **Figures 3, 4, and 5** the FE-SEM images are reported for the two different configurations, oriented and not oriented, for the composite with the highest amount of both fillers: respectively 15% of nickel (Figures 3 and 4) and 5% of CNTs (Figure 5).

Upon the applied external magnetic field, the nickel particles aligned through the direction of the magnetic vectors, therefore creating an uninterrupted thermal path along with the sample section. FE-SEM magnification in Figure 3a,b shows the success orientation of the fillers, underlined by the red arrows. Meanwhile, the sample cured without the applied external magnetic field and therefore with a not oriented configuration of nickel particles did not show the formation of a continuous path (Figure 4). This may contribute to the limited increase of  $k$  (see Section 3.4.) for the not oriented dispersion of the conductive fillers. Nevertheless, no big aggregations were noticed confirming the achievement of good mixing. The interaction between the matrix and the fillers is also remarkable since no discontinuities at the interface were noticed.

The sample containing different percentages of CNTs(Ni) fillers showed also good interaction with the magnetic field due to the magnetic sensitivity of the nickel atoms spread on the carbon nanotubes' external surface. Figure 5a,b shows a preferential perpendicular direction with respect to the fracture direction, which was preferential for the majority of CNTs and influenced by the application of the magnetic field. However, a better observation of Figure 5a,b shows domains with an alternating presence of CNTs(Ni), and therefore with a discontinuity along the sample surface. This could affect the final properties of the composite because no continuous path is noticed for this type of fillers and can contribute to explaining the result obtained for thermal conductivity (Section 3.4.).

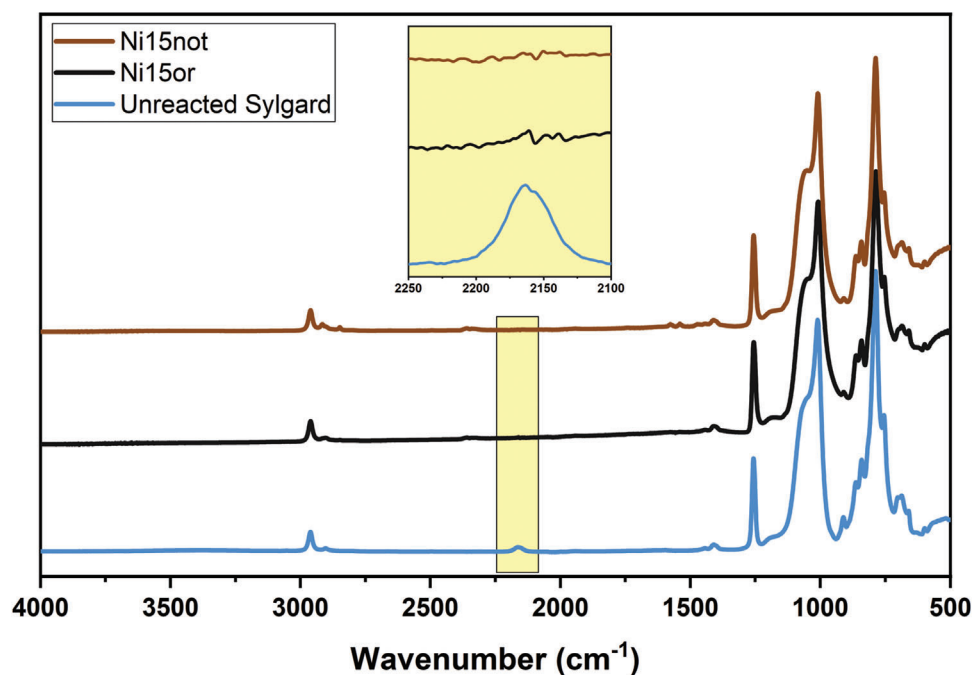


**Figure 2.** ATR spectra of the pristine Sylgard before the curing process (blue line), and of the composites with the 15% of nickel particles obtained upon thermal treatment (70 °C, 1 h). The formulation containing 15% of nickel particles not oriented (Ni15\_not) is plotted in brown line, while the formulation containing 15% of nickel particles oriented (Ni15\_or) is plotted in black line. Magnification on the interested wavenumbers shows complete disappearance of the peak at 2160  $\text{cm}^{-1}$  related to the Si-H group.

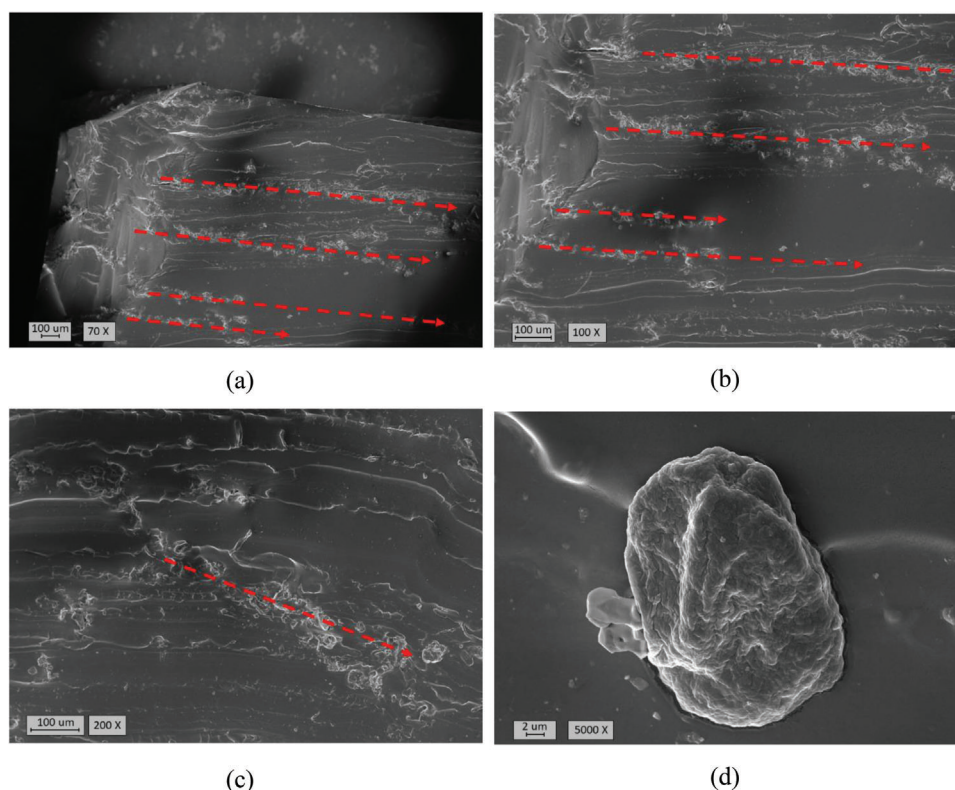


**Figure 3.** SEM analysis of the surface fracture of the composite with 15 vol% of Ni in the oriented a configuration. The a) image and b) enlightened the oriented conformation of the Ni particles obtained with the magnetic field. The red arrows indicate the direction of orientation. Picture c) is obtained with 200x and d) is a zoom of a Ni particle obtained with 5000x.



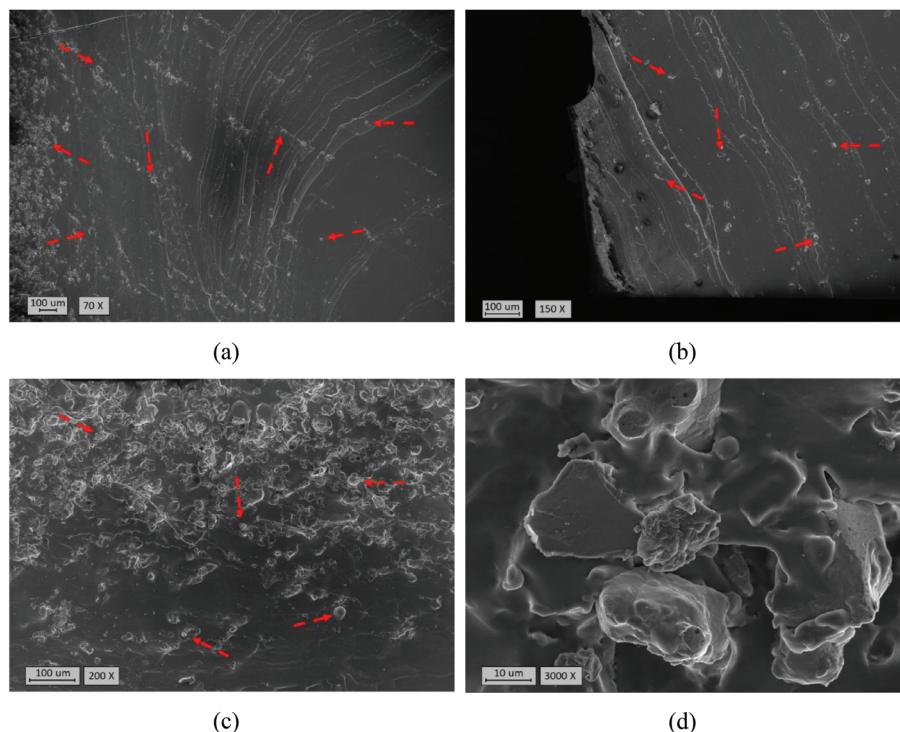


**Figure 4.** SEM analysis of the surface fracture of the composite with 15 vol% of Ni in the not oriented configuration. The image a) is obtained at 70X while the b) is at 150X. It can be noticed that the particles are randomly oriented without a preferential orientation. c) Was at 200X and d) the zoom on a Ni particle is done at 3000X.

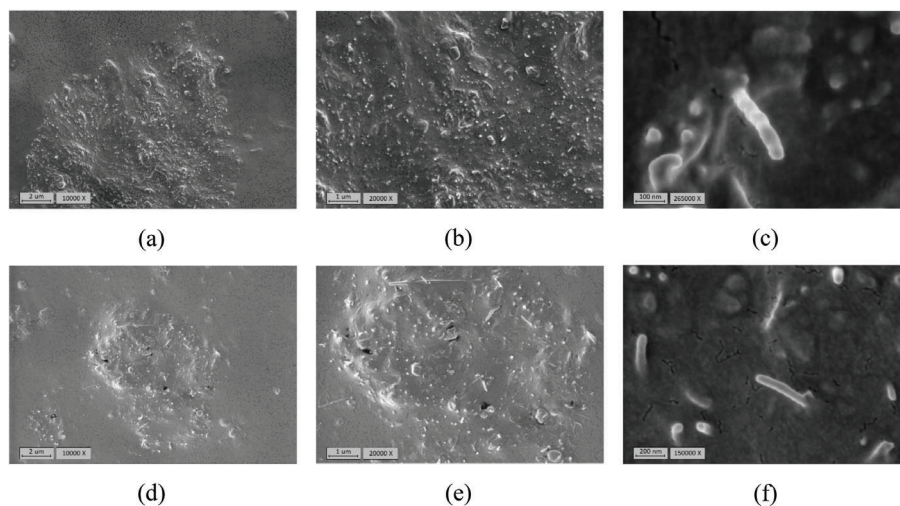


**Figure 5.** SEM images for oriented structure (CNT(Ni)5\_or) obtained at different zoom: a) 10 000X; b) 20 000X and c) 265 000X. d-f) Reported the not oriented configuration (CNT(Ni)5\_not) obtained without the application of a magnetic field.

Instead, Figure 5d,e reports the result of samples cured without an applied magnetic field and therefore with visible casual orientations of the fillers.

### 2.3. Thermo-Mechanical Properties

Dynamic mechanical thermal analysis (DMTA) measurements were carried out to evaluate the influence of the filler disper-

sion and orientation on the thermo-mechanical properties of the cured PDMS composites. In **Figures 6 and 7**,  $\tan\delta$  curves (the ratio of the loss modulus to the storage modulus) are reported, and the glass transition temperature is taken as the temperature that corresponds to the peaks of the  $\tan\delta$  curve. As it can be noticed, the addition of the fillers induced a slight increase of the final  $T_g$ , as also widely reported in literature DMTA measurements were carried out to evaluate the influence of the filler dispersion and orientation on the thermo-mechanical properties of

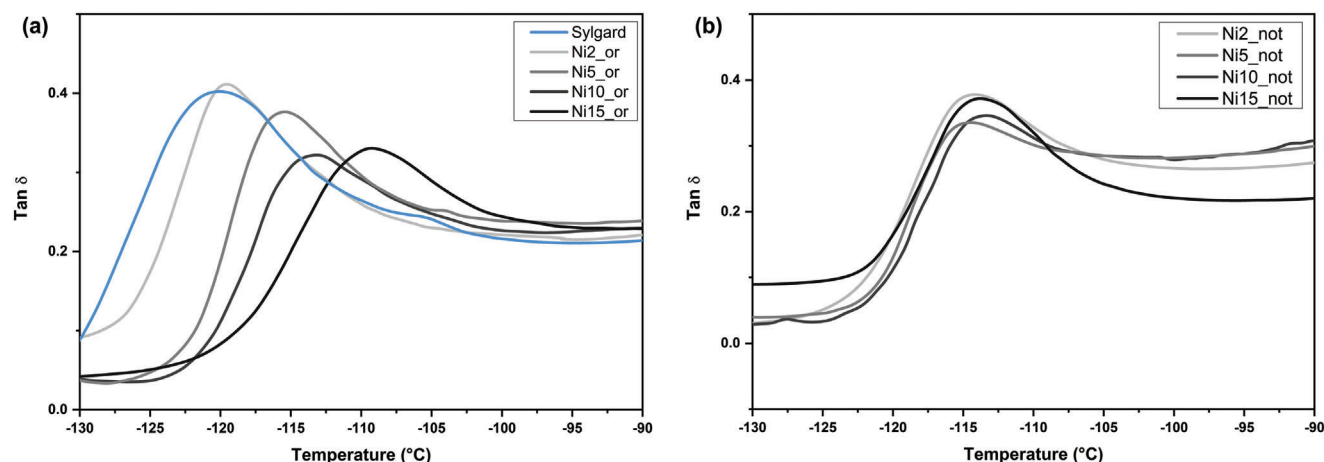


**Figure 6.** DMTA analysis.  $\text{Tan}\delta$  curves obtained for the tested composites with Ni particles. a) Oriented structures; b) Not oriented configurations.

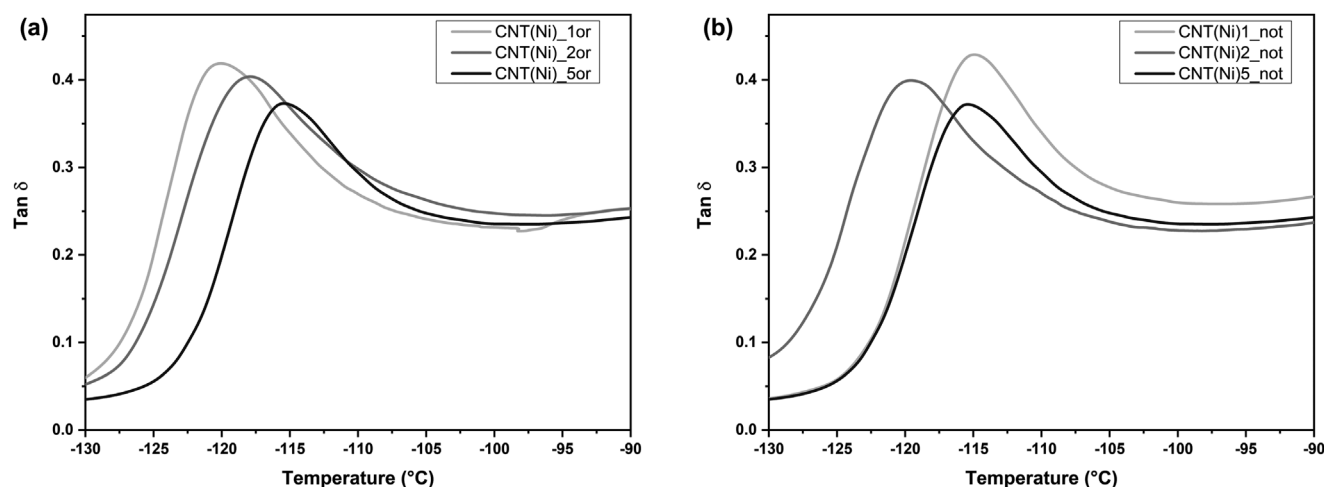


**Figure 7.**  $\text{Tan}\delta$  curves obtained for Sylgard-CNT(Ni) composite. a) Oriented configurations; b) Not oriented structure.

the cured PDMS composites. In Figures 6 and 7,  $\text{Tan}\delta$  curves (the ratio of the loss modulus to the storage modulus) are reported, and the glass transition temperature is taken as the temperature that corresponds to the peaks of the  $\text{Tan}\delta$  curve. As it can be noticed, the addition of the fillers induced a slight increase of the final  $T_g$ , as also widely reported in literature<sup>[2,7,10]</sup> which could be attributed to an hindrance effect of the filler on the motion of the polymer chains. Moreover, considering the orientated configurations, a larger increase can be noticed when the filler is oriented (see data collected in **Table 1**). This could be justified considering that the orientation can further hinder the polymer chain motion, especially through the alignment direction of the fillers. This effect was measured for both Ni particles and CNT(Ni) fillers (Figures 6 and 7).

The effect of the filler dispersion on the mechanical properties of the PDMS composites was further confirmed by means of tensile analysis. **Figure 8** and **Figure 9** clearly show different Stress (MPa)-Strain curves obtained for the composite samples compared to the pristine PDMS matrix. Indeed, the stiffness of

the composite increases proportionally to the added amount of metal or carbon fillers.

The effect of the orientation in terms of mechanical properties and young modulus is shown in **Figure 10**. The investigation put in evidence that the alignment induces a higher increase of the modulus compared to a composite with a not oriented configuration. In fact, considering two composites with the same amount of filler, for instance with 10% of Ni particles, the oriented structure (Ni10\_or) has a modulus of 2.74 MPa compared to 2.35 MPa of modulus measured for the not oriented structure (Ni10\_not). This higher stiffness is in accordance with the differences in the  $\text{Tan}\delta$  curve and in the glass transition temperature ( $T_g$ ) that were previously discussed.<sup>[27]</sup> The higher stiffness is clearly visible in the reduction of the elongation at the break measured for all composites. Indeed, if the pristine Sylgard measures elongation at break close to 200% of the initial sample dimension, the composite structures show a visible reduction of the maximum strain. The composites with CNT(Ni) has an elongation ranging from 185% to 140% respectively passing from 1

**Table 1.** Results obtained from the DMTA analysis and tensile test.  $T_g$  was evaluated as  $\tan\delta$  peak from DMTA analysis.  $E$  is the slope evaluated until 20% of deformation, Tensile strength at break and Elongation at break were evaluated from the tensile measurements.

Acronym	$T_g$ [°C] <sup>a)</sup>	$E$ [MPa] <sup>b)</sup>	Tensile strength at break [MPa] <sup>b)</sup>	Elongation at break [%] <sup>b)</sup>
Sylgard	-121 ± 2	0.83 ± 0.03	1.54 ± 0.03	200 ± 5
Ni2_not	-115 ± 2	1.02 ± 0.04	1.05 ± 0.04	78 ± 2
Ni5_not	-114 ± 2	2.00 ± 0.01	2.14 ± 0.01	82 ± 5
Ni10_not	-115 ± 2	2.35 ± 0.08	2.25 ± 0.08	76 ± 4
Ni15_not	-114 ± 1	4.00 ± 0.06	2.92 ± 0.06	59 ± 6
Ni2_or	-119 ± 2	1.52 ± 0.05	1.68 ± 0.07	87 ± 5
Ni5_or	-115 ± 2	1.77 ± 0.06	2.56 ± 0.04	111 ± 4
Ni10_or	-112 ± 2	2.74 ± 0.03	2.11 ± 0.03	61 ± 6
Ni15_or	-108 ± 1	5.55 ± 0.05	3.06 ± 0.05	55 ± 5
CNT(Ni)1_not	-115 ± 2	1.53 ± 0.01	1.53 ± 0.01	171 ± 4
CNT(Ni)2_not	-119 ± 2	1.57 ± 0.01	1.57 ± 0.01	158 ± 6
CNT(Ni)5_not	-115 ± 2	1.58 ± 0.01	1.58 ± 0.01	152 ± 5
CNT(Ni)1_or	-119 ± 2	1.49 ± 0.06	1.49 ± 0.06	185 ± 4
CNT(Ni)2_or	-117 ± 2	1.60 ± 0.05	1.60 ± 0.05	165 ± 6
CNT(Ni)5_or	-115 ± 2	1.87 ± 0.03	1.87 ± 0.03	140 ± 5

<sup>a)</sup> measured by DMTA; <sup>b)</sup> measured by tensile test.

to 5 vol% of the CNT(Ni) content. However, it is clear again how the introduction of metal particles modifies more strongly the behavior of the pristine polymer which reaches a maximum value of 111% already for the 2 vol% of oriented nickel particles content. This result is in agreement with the DMTA analysis and can be explained by the difference in shape, dimension, and adhesion to the polymer matrix, for the nickel particles compared to the nickel coated carbon nanotubes. An exhaustive overview of all the data regarding  $E$  (elastic modulus), elongation at break, and tensile strength at break is reported in Table 1.

The PDMS crosslinked composites were tested by means of a Hot-Disk to investigate the effect of the two fillers and the magnetic-oriented structures on the anisotropic thermal conduc-

tivity ( $k$ ). Figure 11 shows that the addition of Ni particles reflects a clear enhancement of  $k$  value compared to the pristine matrix, passing from 0.18 W mK<sup>-1</sup> of the pristine structure to 1.44 W mK<sup>-1</sup> of the sample containing 15 vol% of nickel particles. Being more conductive than the PDMS matrix, nickel particles act as a preferential thermal path, therefore increasing the overall anisotropic thermal conductivity. Thus, a continuous path of the nickel particles inside the PDMS network would theoretically guarantee a continuous thermal path inside the polymer network, increasing the overall  $k$  value in that direction. In this regard, Figure 11 clearly shows that comparing samples with the same filler volume percentages, the orientated configurations showed higher anisotropic  $k$  values. For example, it was possible to achieve an increase of 2.9 times, by orienting the nickel particles for the sample containing 10 vol% of filler, producing a total increase of 715% compared to the pristine matrix. In the measured set of samples, the highest  $k$  was reached with the formulation containing 15 vol% of nickel particles with a  $k$  value of 1.44 W mK<sup>-1</sup>, which results in an overall increase of about 800% compared to the pristine Sylgard matrix. These results demonstrate how magnetically oriented fillers represent a simple and effective way for establishing a thermal preferential path, thus reducing the thermal resistance of a polymer matrix. These results showed a higher increase of the overall anisotropic  $k$  value compared to previous studies.<sup>[21,22]</sup> (Figure 12)

A similar trend among oriented and not oriented fillers can be noticed also for the composites containing CNT(Ni) carbon nanotubes. However, a lower  $k$  value was measured for the sample containing the same volume percentage of CNT(Ni)s and nickel particles, both in the oriented and not oriented configurations. For instance, the composite containing 5 vol% of oriented nickel particles (Ni5\_or) has a  $k$  value above 1 W mK<sup>-1</sup>, while the composite containing 5 vol% of oriented nickel-coated carbon nanotubes (CNT(Ni)5\_or) has a  $k$  coefficient of around 0.5 W mK<sup>-1</sup>. Despite this result could appear in contradiction with the higher  $k$  value of carbon nanotubes compared to nickel particles, it could be explained considering the better formation of a continuous path for the nickel particles, as evidenced in scanning electron microscopy (SEM) analysis. In fact, the formation of alternating domains, with and without CNTs(Ni), drastically reduces the

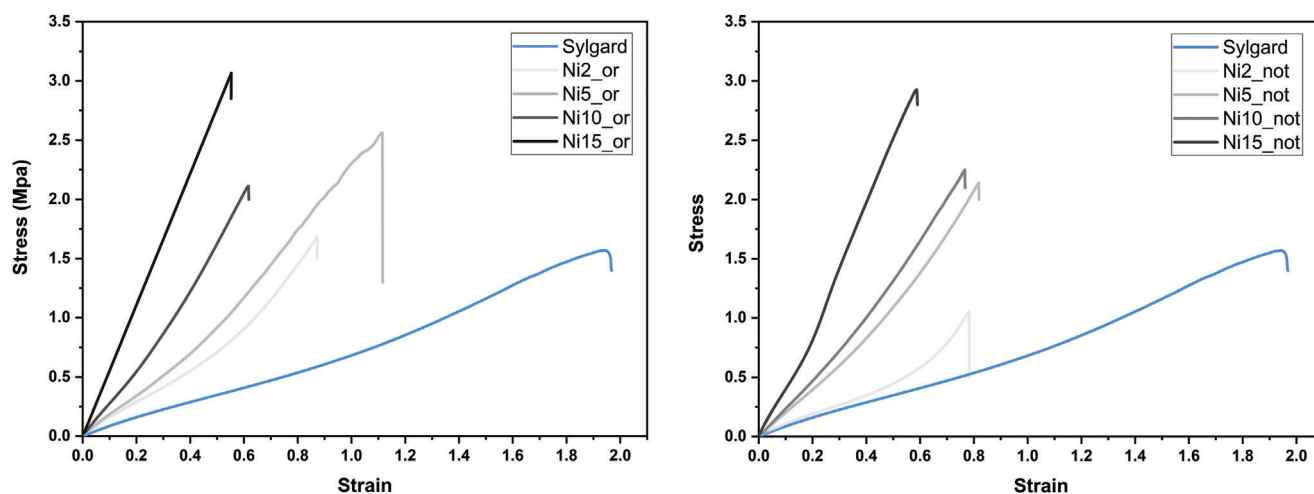


**Figure 8.** Stress–strain curves obtained from tensile analysis of the composites with Ni metal particles.



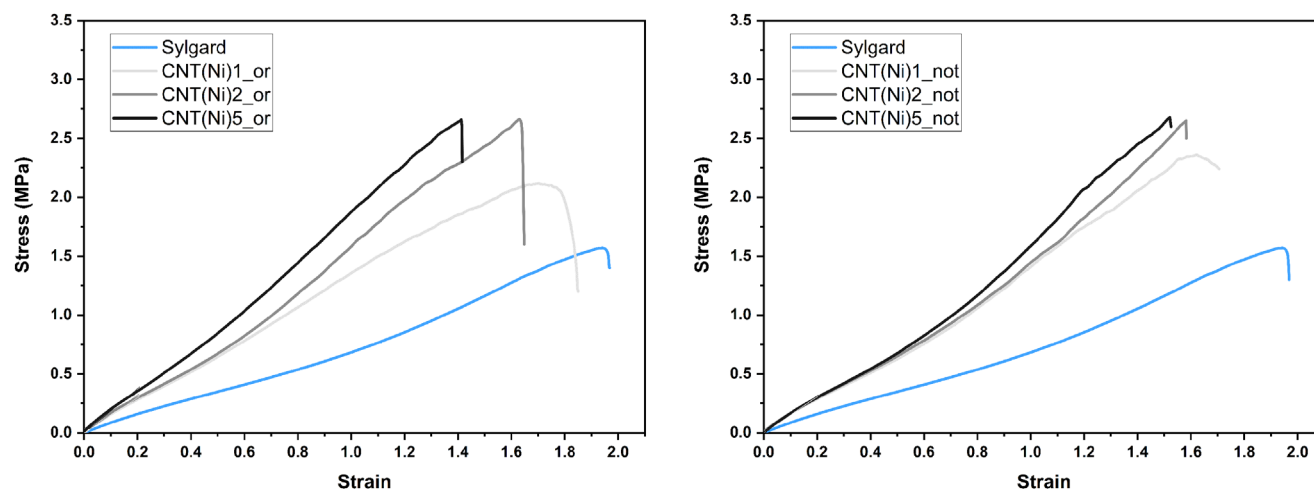


**Figure 9.** Stress–strain curves obtained from tensile analysis of the CNT(Ni) composites.

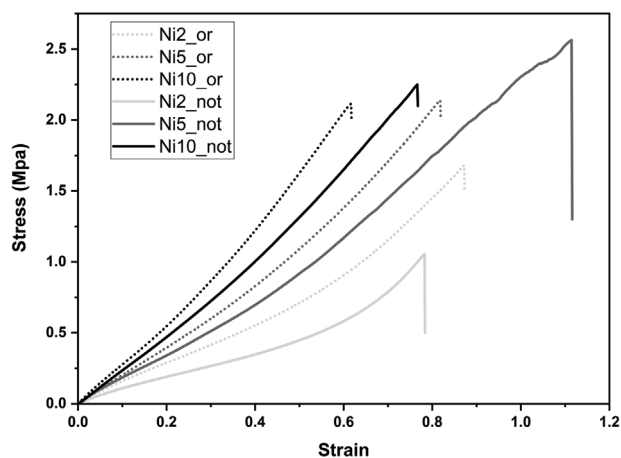


**Figure 10.** Stress–strain curves obtained from the composite with Ni particles. In this plot, it is highlighted the effect of the orientation of the particles on the final mechanical properties.

potential of the higher carbon nanotubes' thermal conductivity, resulting in a lower overall  $k$  value. In this regard, a higher overall  $k$  value could be achieved both by increasing the CNTs(Ni) content and also by improving the dispersion of CNTs(Ni) into the polymer matrix, thus promoting the creation of a continuous thermal path inside the PDMS network.

### 3. Conclusion

This work gives an insight into the effect of magnetic-oriented nickel particles and nickel-coated nanotubes for the enhancement of the thermal conductivity of PDMS composites. The fillers' orientation occurs in the liquid formulation under the effect of two magnets set parallel to the sample surface. Upon thermal curing at 70 °C, FE-SEM images confirm the nickel particles' orientation in a parallel disposition to the magnetic field lines. DMTA and tensile analysis shows an important change of the thermo-mechanical properties with the fillers content increase, but only slight changes for the samples with different fillers dis-

position (magnetic-oriented compared to not oriented). Finally, the use of a magnetic field to control the orientation of the fillers give interesting results in terms of thermal conductivity with a further increase of 2.9 times compared to the composites with a not oriented configuration. Therefore, the fillers orientation significantly enhances the thermal properties of the pristine polymer (7.9 times for the 15 % oriented compared to the pristine) maximizing the effect of the filler exploiting its attitude of orientation if magnetic field is applied. Therefore, this allowed to limit the addition of the filler without significantly affecting mechanical properties as aforementioned. However, despite the good results obtained for the nickel particles, nickel-coated multi walled carbon nanotubes did not give enthusiastic results in terms of thermal conductivity. In a following step, we will work in improving the interface between the fillers and polymeric matrix, and also in better controlling the dispersion of the nickel-coated carbon nanotubes.

### 4. Experimental Section

**Materials:** Polydimethylsiloxane Sylgard 184 (Sylgard) (SYLGARD 184, Dow Corning Corporation), was used as a precursor of the polymeric matrix. For the curing step, it was mixed in ratio 10:1 with a curing agent, given as Part B of the formulation. Nickel (Ni) particles with an average size of 45  $\mu\text{m}$  and a purity of 99.8% were purchased from Sigma-Aldrich. Nickel-coated carbon nanotubes, CNT(Ni) with a diameter of 28–48  $\mu\text{m}$  with purity of 99% were purchased from Nanografi. The fillers were used as received without further purification.

SEM analysis was carried out on the filler in order to confirm the data and to verify the average dimension. The **Figure 13** shows the images for the fillers used in the study: Ni powder and CNT(Ni). The average dimension of Ni particles was  $39 \pm 9 \mu\text{m}$  evaluated with an average of 20 particles. The SEM analysis highlights the irregular shape of the filler. The CNT(Ni) had an average diameter of  $26 \pm 5 \text{ nm}$ . The distribution of the measured filler is reported in the **Figure 14**.

**Formulation Preparation and Thermal Curing:** A typical formulation was prepared by first adding the fillers to the Sylgard liquid formulation with a weight percentage according to **Table 2**. Once the fillers were added, the formulation was mixed for 5 min at 500 rpm with DLS Digital Overhead Stirrer (VELP SCIENTIFICA). In a second step, the curing agent was added in a ratio of 10:1 (Sylgard: Curing agent), and the formulations were stirred

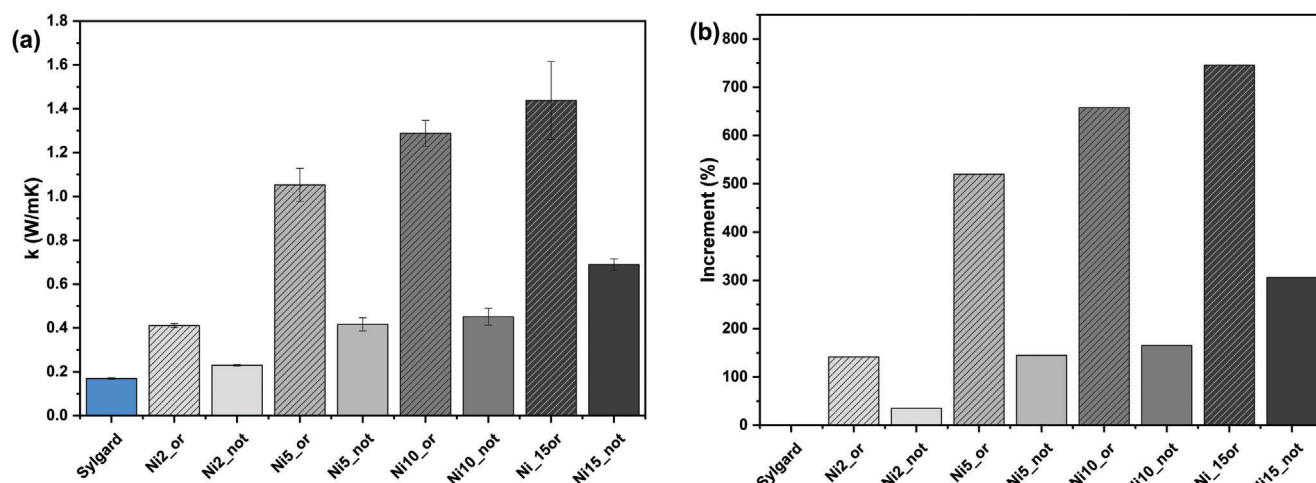


**Figure 11.** a) Thermal conductivity for the composites with Ni particles; b) Increment of the  $k$  value (right side) evaluated with respect to the value obtained for the Sylgard in the used curing condition (70 °C, 1 h).

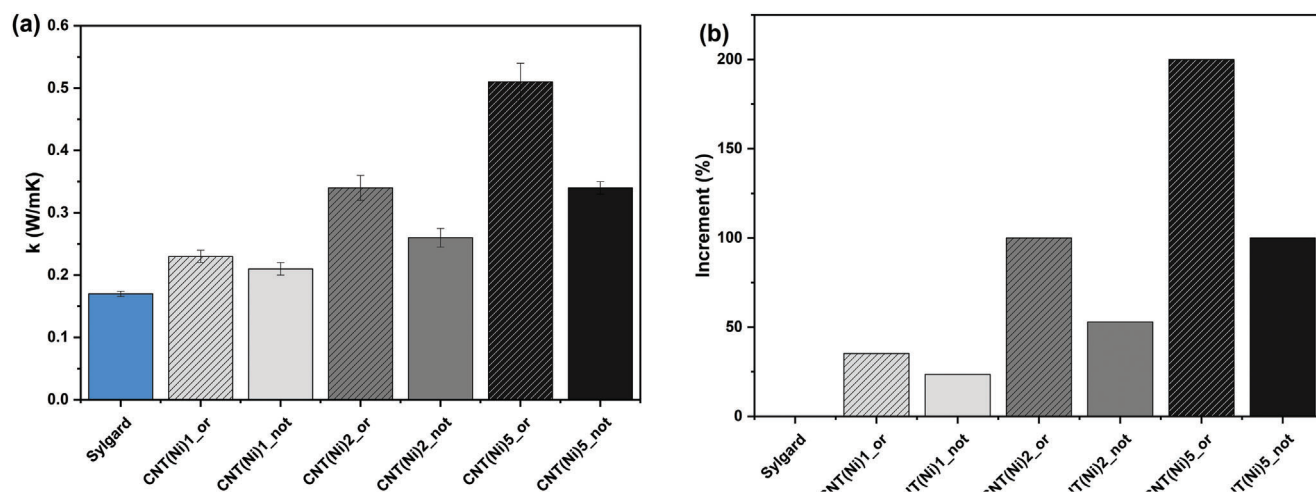


**Figure 12.** a) Thermal conductivity measured for the different composites with CNT(Ni); b) percentage (%) of increment compared to the pristine Sylgard matrix.

once more for 2 min. The addition of the curing agent in a second step allowed a homogeneous mixing of the Sylgard-fillers formulations without any risk of premature curing during the mixing step. Subsequently, the prepared formulations were cast in a Teflon mold, and vacuum degassing of about 15 min was applied. Two different types of samples were obtained and specifically either with an oriented filler and a not orientated configuration. The orientation was achieved by the application of a magnetic field during the curing stage in the aim to align the filler parallel to the magnetic field. The curing was performed in an oven, in which molds were put in for 1 h at 70 °C. The magnets used for orienting the fillers in the polymer matrix were an S-60-05-N, Webcraft GmbH, Gottmadingen, German, made of a metal alloy of neodymium, iron, and boron (NdFeB), with a round shape of 60 mm diameter and 5 mm thickness and with an attraction force of 21 kg with a remanence of 1.29–1.32 T. Different samples were prepared by respecting the dimensions required for the analyses.

**Characterization:** Rheology—The thermal curing was investigated by rheological test by means of an Anton Paar MC 302 rheometer. The conditions for the tests were the following: frequency of 1 Hz and strain of 1% with disposable smooth aluminum parallel plate (diameter of 25 mm) and a distance between the plates of 200  $\mu$ m which corresponds approximately to about 200–300 mg of the liquid formulation. In order to simu-

late the oven condition in which all the samples were cured, the rheology measurement was conducted by setting a ramp of 4 °C min<sup>-1</sup> from room temperature up to 70 °C, followed by isothermal curing conditions at 70 °C for 1 h.

**ATR-FTIR**—The attenuated total reflection Fourier transform infrared spectroscopy (ATR-FTIR) spectra were collected by using a Perkin Elmer Spectrum 2000 FTIR (Waltham, Massachusetts) equipped with attenuated total reflectance (ATR) accessory. The spectra were collected between 4000 and 500 cm<sup>-1</sup>, 32 scans were recorded for each sample and the resolution was set as 4 cm<sup>-1</sup>. The thermal curing was investigated by following the peak of Si-H groups at 2160 cm<sup>-1</sup>, which belongs to the adopted thermal initiator.

**SEM:** SEM—The dispersion of the different fillers in the different composites was evaluated through scanning electron microscopy performed by means of FESEM, Zeiss Supra 40, Oberkochen, Germany. The surface fracture samples were coated with a 5 nm layer of gold and observed with the FESEM operating at 7.5 kV with aperture size of 30  $\mu$ m for the composite with nickel particles and 2.0 kV for the composite with the nanotubes.

**DMTA**—Crosslinked samples of 20 × 20 × 4 mm<sup>3</sup> (length × width × thickness) were prepared and the DMTA analyses were performed by

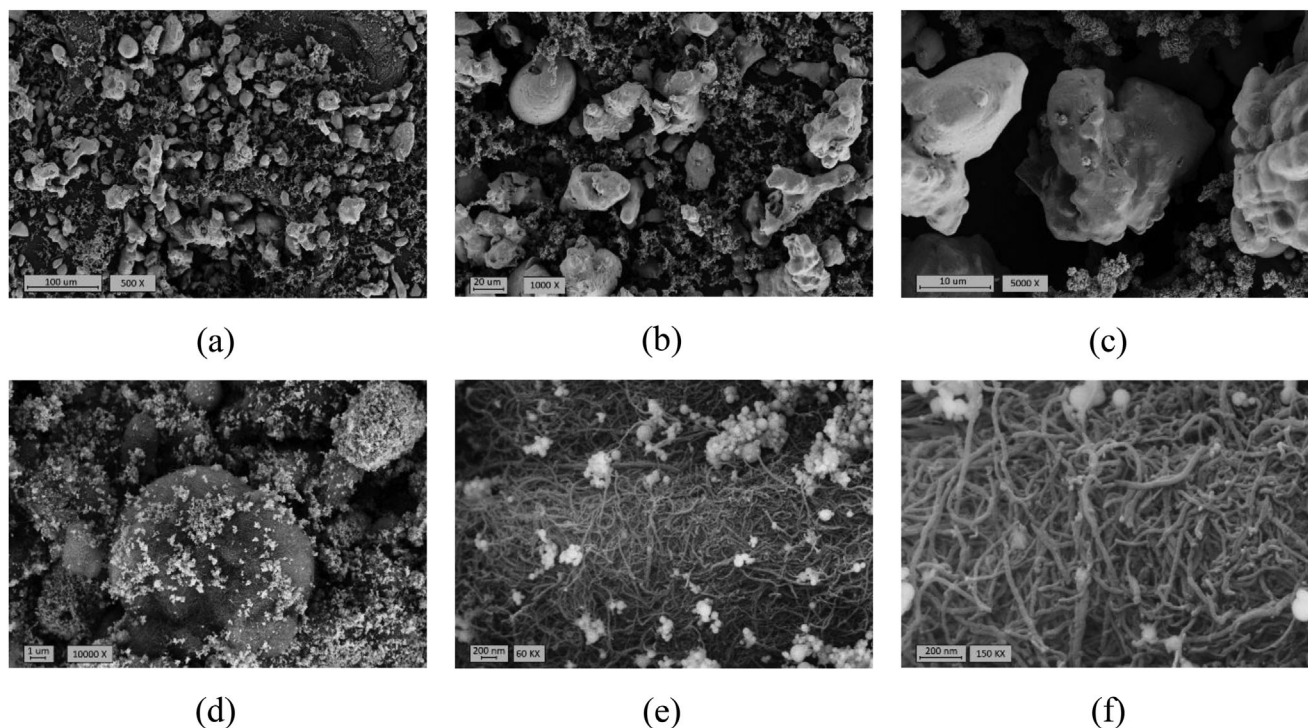


**Figure 13.** SEM images for Ni powder obtained at different zoom: a) 500x; b) 1000x, and c) 5000x. d–f) Reported the CNT(Ni) at different magnification: 10, 60, and 150 KX.

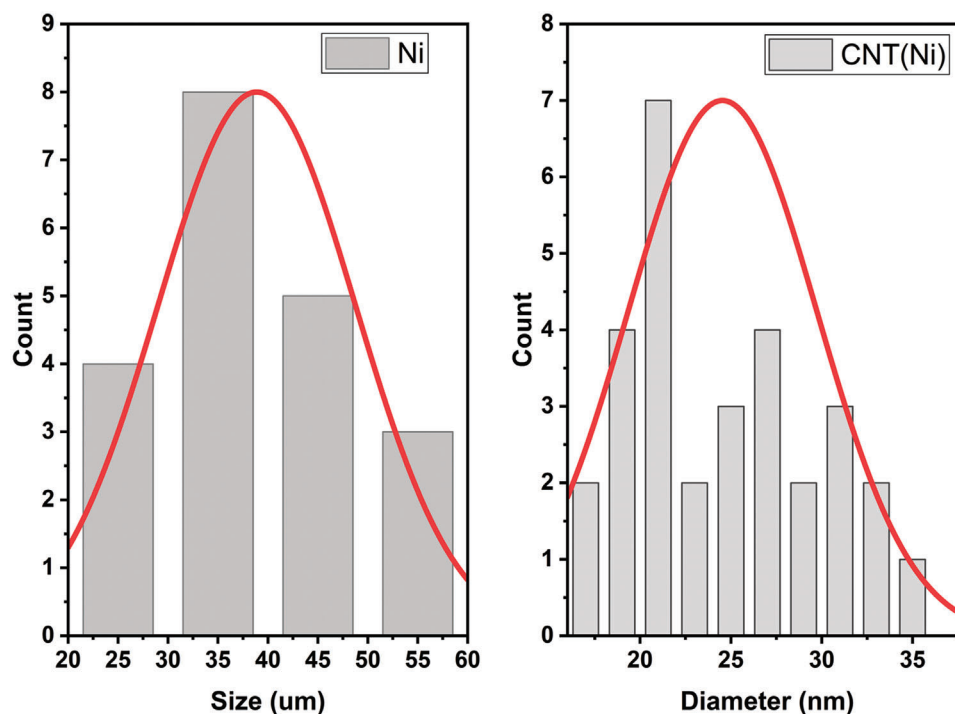


**Figure 14.** Distribution of the measured Ni particles and CNT(Ni).



**Table 2.** Composition of the tested formulations with the two different fillers (Ni and CNT(Ni)), the adopted volume percentage (vol%) and configuration oriented (or) and not oriented (not).

Acronym	Type of filler	Filler [vol%]	Filler [wt%]
Sylgard	/	0.00	0.00
Ni2_not	Nickel powder (<45 $\mu\text{m}$ )	2.00	14.75
Ni5_not	Nickel powder (<45 $\mu\text{m}$ )	5.00	30.80
Ni10_not	Nickel powder (<45 $\mu\text{m}$ )	10.00	48.50
Ni15_not	Nickel powder (<45 $\mu\text{m}$ )	15.00	59.95
Ni2_or	Nickel powder (<45 $\mu\text{m}$ )	2.00	14.75
Ni5_or	Nickel powder (<45 $\mu\text{m}$ )	5.00	30.80
Ni10_or	Nickel powder (<45 $\mu\text{m}$ )	10.00	48.50
Ni15_or	Nickel powder (<45 $\mu\text{m}$ )	15.00	59.95
CNT(Ni)1_not	CNT coated with Ni	1.00	2.54
CNT(Ni)2_not	CNT coated with Ni	2.00	5.03
CNT(Ni)5_not	CNT coated with Ni	5.00	12.00
CNT(Ni)1_or	CNT coated with Ni	1.00	2.54
CNT(Ni)2_or	CNT coated with Ni	2.00	5.03
CNT(Ni)5_or	CNT coated with Ni	5.00	12.00

means of the Triton Technology instrument (Keyworth, Nottingham, Great Britain). Liquid nitrogen was used to cool down the test chamber to permit to set an initial temperature of  $-140\text{ }^{\circ}\text{C}$ , and the test was performed with a heating rate of  $3\text{ }^{\circ}\text{C min}^{-1}$  until  $-90\text{ }^{\circ}\text{C}$ . The tensile stress applied was with a frequency of 1 Hz and displacement of  $20\text{ }\mu\text{m}$ . The tensile stress was applied in parallel direction with respect to the orientation of the filler.

**Tensile Test**—Crosslinked samples of  $60 \times 6 \times 0.5\text{ mm}^3$  (length  $\times$  width  $\times$  thickness) were prepared, in line with the ASTM D882 standard for thin-film<sup>[28]</sup> and the tensile test was performed using a tensile instrument (MTS QTestTM/10 Elite, MTS System Corporation) combined with a measurement software (TestWorks 4, MTS System Corporation). The parameters for the test were set as follows: test speed at  $50\text{ mm min}^{-1}$  and data acquisition rate at 50 Hz. A 50 N load cell was used to perform the test, which was carried out five times for every sample. Young's modulus, ultimate tensile strength (UTS), and elongation at break were measured. The tensile test was done applying the stress in parallel direction with respect to the orientation of the filler.

**Thermal Analysis**—The thermal conductivity ( $k$ ) of the different composites were investigated by means of TPS2500S, Hot Disk AB (Walthman, USA) was equipped with a sensor 5465, Kapton sensor, Hot Disk AB, (Walthman, USA) with 3.189 mm of radius. The composites were tested through the transient plane heat source method according to ISO 22007-2.<sup>[29]</sup> Two samples with parallelepiped shape ( $20 \times 20 \times 4\text{ mm}^3$  length  $\times$  width  $\times$  thickness), for each material, were taken in contact with the sensor and they were placed in a container with a temperature controller (Haake AC200, Thermo Scientific Inc., Walthman, USA), which set the temperature at  $23 \pm 0.01\text{ }^{\circ}\text{C}$ . The measured time was 2 s, and it started after the impulse of 30 mW. The conductive value is the average obtained after 25 measures.

## Acknowledgements

Open Access Funding provided by Politecnico di Torino within the CRUI-CARE Agreement.

## Conflict of Interest

The authors declare no conflict of interest.

## Data Availability Statement

The data that support the findings of this study are available from the corresponding author upon reasonable request.

## Keywords

magnetic orientation, nickel, silicon, thermal conductivity, thermal-curing

Received: June 22, 2022  
Revised: September 12, 2022  
Published online:

- [1] F. Sarvar, D. C. Whalley, P. P. Conway, *2006 1st Electron. Syst. Technol. Conf.* **2006**, 2, 1292.
- [2] L. Pezzana, et al., *Nanomaterials* **2021**, 11.
- [3] H. Chen, V. V. Ginzburg, J. Yang, Y. Yang, W. Liu, Y. Huang, L. Du, B. Chen, *Prog. Polym. Sci.* **2016**, 59, 41.
- [4] C. Huang, X. Qian, R. Yang, *Mater. Sci. Eng., R* **2018**, 132, 1.
- [5] Z. Huang, et al., *Polymers (Basel)* **2021**, 13, 1.
- [6] J.-U. k Ha, J. Hong, M. Kim, J. K. Choi, D. W. Park, S. E. Shim, *Kobunja Kwahak Kwa Kisul* **2013**, 37, 722.
- [7] M. Sangermano, N. Razza, G. Graham, I. Barandiaran, G. Kortaberria, *Polym. Int.* **2017**, 66, 1935.
- [8] Y. Guo, K. Ruan, X. Shi, X. Yang, J. Gu, *Compos. Sci. Technol.* **2020**, 193, 108134.
- [9] X. Huang, P. Jiang, T. Tanaka, *IEEE Electr. Insul. Mag.* **2011**, 27, 8.
- [10] G. Riccucci, et al., *Appl. Sci.* **2021**, 11.
- [11] K. Sanada, Y. Tada, Y. Shindo, *Composites, Part A* **2009**, 40, 724.
- [12] A. Boudenne, L. Ibos, M. Fois, J. C. Majesté, E. Géhin, *Composites, Part A* **2005**, 36, 1545.
- [13] A. Tessema, D. Zhao, J. Moll, S. Xu, R. Yang, C. Li, S. K. Kumar, A. Kidane, *Polym. Test.* **2017**, 57, 101.
- [14] Z. Han, A. Fina, *Prog. Polym. Sci.* **2011**, 36, 914.
- [15] H. Huang, C. H. Liu, Y. Wu, S. Fan, *Adv. Mater.* **2005**, 17, 1652.
- [16] C. H. Liu, H. Huang, Y. Wu, S. S. Fan, *Appl. Phys. Lett.* **2004**, 84, 4248.
- [17] M. J. Biercuk, M. C. Laguno, M. Radosavljevic, J. K. Hyun, A. T. Johnson, J. E. Fischer, *Appl. Phys. Lett.* **2002**, 80, 2767.
- [18] S. Lantean, G. Barrera, P. M. Tiberto, C. F. Pirri, M. Sangermano, G. Rizza, I. Roppolo, *Adv. Mater. Technol.* **2019**, 4, 1900505.
- [19] S. Lantean, I. Roppolo, M. Sangermano, M. Hayoun, H. Damak, G. Rizza, *Addit. Manuf.* **2021**, 47, 102343.
- [20] P. S. Goh, A. F. Ismail, B. C. Ng, *Composites, Part A* **2014**, 56, 103.
- [21] A. Boudenne, Y. Mamunya, V. Levchenko, B. Garnier, E. Lebedev, *Eur. Polym. J.* **2015**, 63, 11.
- [22] J. Su, X. Liu, M. Charmchi, H. Sun, *Int. J. Heat Mass Transfer* **2016**, 97, 645.
- [23] K. Kim, J. Kim, *Int. J. Therm. Sci.* **2016**, 100, 29.
- [24] J.-Y. Chung, J.-G. Lee, Y.-K. Baek, P.-W. Shin, Y.-K. Kim, *Composites, Part B* **2018**, 136, 215.
- [25] B. Wright, D. Thomas, H. Hong, L. Groven, J. Puszyński, E. Duke, X. Ye, S. Jin, *Appl. Phys. Lett.* **2007**, 91, 173116.
- [26] M. Liu, H. Younes, H. Hong, G. P. Peterson, *Polymer (Guildf)* **2019**, 166, 81.
- [27] S. Lee, S. Ryu, *Eur J Mech A Solids* **2018**, 72, 79.
- [28] ASTM, [www.Astm.Org](http://www.Astm.Org), <https://doi.org/10.1520/D0882-18> (accessed: 2002).
- [29] ISO 22007-2, <https://www.iso.org/obp/ui/#iso:std:iso:22007:-2:ed-2:v1:en> (accessed: 2015).